

# LoLA: Low-Rank Linear Attention With Sparse Caching

**Luke McDermott**  
UC San Diego  
lmcdermo@ucsd.edu

**Robert W. Heath Jr.**  
UC San Diego  
rwheathjr@ucsd.edu

**Rahul Parhi**  
UC San Diego  
rahul@ucsd.edu

## Abstract

Transformer-based large language models suffer from quadratic complexity at inference on long sequences. Linear attention methods are efficient alternatives, however, they fail to provide an accurate approximation of softmax attention. By additionally incorporating sliding window attention into each linear attention head, this gap can be closed for *short* context-length tasks. Unfortunately, these approaches cannot recall important information from long contexts due to “memory collisions”. In this paper, we propose LoLA: Low-rank Linear Attention with sparse caching. LoLA separately stores additional key-value pairs that would otherwise interfere with past associative memories. Moreover, LoLA further closes the gap between linear attention models and transformers by distributing past key-value pairs into three forms of memory: (i) recent pairs in a local sliding window; (ii) difficult-to-memorize pairs in a sparse, global cache; and (iii) generic pairs in the recurrent hidden state of linear attention. As an inference-only strategy, LoLA enables pass-key retrieval on up to 8K context lengths on needle-in-a-haystack tasks from RULER. It boosts the accuracy of the base subquadratic model from 0.6% to 97.4% at 4K context lengths, with a  $4.6\times$  smaller cache than that of Llama-3.1 8B. LoLA demonstrates strong performance on zero-shot commonsense reasoning tasks among 1B and 8B parameter subquadratic models. Finally, LoLA is an extremely lightweight approach: Nearly all of our results can be reproduced on a single consumer GPU.

## 1 Introduction

Transformer-based large language models (LLMs) rely on storing all past tokens in an ever-growing key-value (KV) cache [47]. This allows future query tokens to access past memories with associative recall, which enables in-context learning [32]. Since no previous information is discarded, the KV cache continues to grow with context length. This eventually leads to a memory bottleneck on long context tasks. As a result, transformers cannot condition next token predictions on arbitrarily long sequences.

Alternative architectures to transformers have been proposed—such as Mamba [21], DeltaNet [41], linear attention [27], and others [3, 45, 51]—to reduce the compute complexity from quadratic to linear. Additionally, these approaches reduce the memory cost from linear to constant. In particular, linear attention removes the exponential dot product in softmax [27]. This effectively collapses the unbounded KV-cache into a fixed-size matrix, which corresponds to a recurrently formed hidden state (i.e., a linear RNN). This constructs a linear associative memory map from keys to values. Past memories can be recalled through a vector-matrix product of an incoming query vector and the hidden state matrix. Linear attention enables constant-cost prediction per token when conditioned on arbitrarily long contexts.

While efficient and flexible, linear attention architectures lag behind transformers in language modeling tasks [52]. This is largely noticeable on tasks leveraging in-context learning [25, 33]. The removal of the exponential dot product allows for non-orthogonal keys to interfere with the hidden state’s learned key-to-value map. This interference impairs associative recall. Previous work used nonlinear query and key activations to improve the exponential dot product approximation [11, 57]. Though, these attempts are essentially performing a low-rank approximation of the infinite-rank exponential dot product kernel.

Additional use of sparse attention [10] can improve linear attention’s low-rank approximation. Previously, LoLCATs [56] exploited locality in natural language by augmenting feature-map-based linear attention with sliding-window attention [1]. Furthermore, this method demonstrates that pretrained Transformers can be distilled into linear attention architectures (see also the concurrent work [5, 6, 49]). The use of distillation and sliding-window attention performs well for short-context tasks. These models, however, struggle to recall critical, long-term facts that fall outside the sliding window.

This raises our fundamental research question:

■ *How can associative memory for language models be improved with a finite memory footprint?*

## Contributions

We present LoLA: Low-rank Linear Attention with sparse caching. LoLA distributes historical tokens into three forms of memory: (i) recent KV pairs are stored in a sliding window cache, (ii) difficult-to-memorize pairs in a sparse global cache, and (iii) all other pairs are placed in a recurrent hidden-state matrix via linear attention. LoLA performs a self-recall check to see which KV pairs disagree with the current hidden state’s linear associative map. LoLA sparsely caches the interfering memories in full-rank. The selection mechanism effectively mitigates memory collisions with a small, constant-sized cache. This inference strategy can be applied on top of previously trained linear attention + sliding window models (e.g., LoLCATs) to significantly improve associative recall. As a result, LoLA extracts stronger language modeling capabilities from the same base model weights.

**Enables Associative Recall.** As a lightweight inference strategy, LoLA enables pass-key retrieval on up to 8K context lengths in needle-in-a-haystack tasks from the RULER benchmark [25]. With a **4.6x smaller** cache than Llama-3.1 8B [20], our approach boosts accuracy from LoLCATs’ **0.6%** to **97.4%** at 4K context lengths with the same model weights. In our ablations, we show that this performance increase cannot be obtained from using a larger sliding window: *global, sparse caching is essential*.

**Improves Language Modeling.** LoLA improves the performance on zero-shot commonsense reasoning tasks from LM Evaluation Harness [17]. LoLA shows superior performance on many tasks among 1B and 8B parameter subquadratic architectures. This demonstrates that effective memory management can boost performance on language modeling tasks.

**Reproducible on Consumer GPUs.** LoLA achieves high performance on an academic budget. Nearly all of our method’s results can be reproduced on a *single* Nvidia RTX 4090.

## 2 Preliminaries

In this section, we review softmax attention through the lens of associative memory. Then, we show how linear attention naturally forms a recurrent hidden state. We address practical implementations for training linear architectures and highlight unresolved drawbacks of previous approaches.

### 2.1 Softmax Attention

Transformers process a sequence of input tokens  $\{x_t\}_{t=1}^n$ , for  $x_t \in \mathbb{R}^d$  [47]. The tokens are transformed into three distinct representations—queries, keys, and values—via trainable weight matrices  $\mathbf{W}_q, \mathbf{W}_k, \mathbf{W}_v \in \mathbb{R}^{d \times d}$ . For a given token  $x_t$ , define

$$\underbrace{q_t = \mathbf{W}_q x_t}_{\text{query}}, \quad \underbrace{k_t = \mathbf{W}_k x_t}_{\text{key}}, \quad \underbrace{v_t = \mathbf{W}_v x_t}_{\text{value}}. \quad (1)$$

Causal attention uses the current query to recall past information from key-value pairs. The similarity between the query  $\mathbf{q}_t$  and key  $\mathbf{k}_i$  is denoted as  $\alpha_{ti} \in (0, 1)$ . This similarity score determines how much value  $\mathbf{v}_i$  is used for the current output token. The output token  $\mathbf{y}_t$  is defined by

$$\mathbf{y}_t = \sum_{i=1}^t \alpha_{ti} \mathbf{v}_i \in \mathbb{R}^d, \quad \text{with} \quad \alpha_{ti} = \frac{\exp(\mathbf{q}_t^\top \mathbf{k}_i / \sqrt{d})}{\sum_{j=1}^t \exp(\mathbf{q}_t^\top \mathbf{k}_j / \sqrt{d})}. \quad (2)$$

The collection of key-value pairs,  $\{(\mathbf{k}_i, \mathbf{v}_i)\}_{i=1}^t$ , forms an associative memory bank [7]. Attention leverages this to learn a non-parametric key-to-value map at inference time. The output token is the predicted value associated with a given query. Softmax attention caches all key-value pairs to perform this non-parametric, or “look-up table”, operation. This leads to an unbounded KV-cache size of  $\mathcal{O}(nd)$  with respect to sequence length  $n$ .

## 2.2 Linear Attention

Linear attention performs a low-rank approximation of the exponential dot product kernel [27]. This enables models to maintain constant-size memory footprints even for infinite sequence lengths. With this kernel approximation,

$$\phi : \mathbb{R}^d \rightarrow \mathbb{R}^D, \quad \text{such that} \quad \exp\left(\frac{\mathbf{q}_t^\top \mathbf{k}_j}{\sqrt{d}}\right) \approx \phi(\mathbf{q}_t)^\top \phi(\mathbf{k}_j), \quad (3)$$

the output token is approximated as

$$\begin{aligned} \mathbf{y}_t^\top &= \sum_{i=1}^t \frac{\exp(\mathbf{q}_t^\top \mathbf{k}_i / \sqrt{d}) \mathbf{v}_i^\top}{\sum_{j=1}^t \exp(\mathbf{q}_t^\top \mathbf{k}_j / \sqrt{d})} \approx \sum_{i=1}^t \frac{\phi(\mathbf{q}_t)^\top \phi(\mathbf{k}_i) \mathbf{v}_i^\top}{\sum_{j=1}^t \phi(\mathbf{q}_t)^\top \phi(\mathbf{k}_j)} = \frac{\phi(\mathbf{q}_t)^\top \left(\sum_{j=1}^t \phi(\mathbf{k}_j) \mathbf{v}_j^\top\right)}{\phi(\mathbf{q}_t)^\top \left(\sum_{j=1}^t \phi(\mathbf{k}_j)\right)} \\ &= \frac{\phi(\mathbf{q}_t)^\top \mathbf{H}_t}{\phi(\mathbf{q}_t)^\top \mathbf{s}_t}. \end{aligned} \quad (4)$$

This creates a hidden state matrix  $\mathbf{H}_t \in \mathbb{R}^{D \times d}$  as the sum of key-value outer products. This effectively bounds the memory cost to  $\mathcal{O}(Dd)$ , constant with respect to sequence length  $n$ . The hidden dimension size  $D$  controls the approximation quality at the cost of computational efficiency. As a linear RNN, the hidden state  $\mathbf{H}_t$  and normalization state  $\mathbf{s}_t \in \mathbb{R}^D$  can be computed recurrently,

$$\mathbf{H}_t = \mathbf{H}_{t-1} + \phi(\mathbf{k}_t) \mathbf{v}_t^\top, \quad \mathbf{s}_t = \mathbf{s}_{t-1} + \phi(\mathbf{k}_t). \quad (5)$$

In this formulation, linear attention treats each associative memory as a rank-one outer product. Rather than building a look-up table, linear attention parameterizes the key-to-value map as a linear function. This is viewed as an online learning problem, where the hidden state fits to the past KV-pairs in context [50].

## 2.3 Efficient Training of Linear Attention

To reduce the training costs, LoLCATs [56] and others [5, 6, 49] recycle large pretrained transformers into linear attention models with knowledge distillation [24]. These approaches minimize the difference between the pretrained transformer’s output  $\mathbf{y}$  (i.e., the teacher) and linear attention’s output  $\hat{\mathbf{y}}$  (i.e., the student). In particular, LoLCATs uses a trainable nonlinear map for  $\phi : \mathbb{R}^d \rightarrow \mathbb{R}^D$ , constructed as

$$\phi(\mathbf{x}) = \left[ \exp(\mathbf{w}_1^\top \mathbf{x}), \dots, \exp(\mathbf{w}_{D/2}^\top \mathbf{x}), \exp(-\mathbf{w}_1^\top \mathbf{x}), \dots, \exp(-\mathbf{w}_{D/2}^\top \mathbf{x}) \right] \in \mathbb{R}^D, \quad (6)$$

with learnable weights  $\mathbf{w}_i \in \mathbb{R}^d$  [57]. This distillation approach freezes all other parameters, adjusting  $\phi$  to minimize the loss

$$\mathcal{L}(\phi) = \sum_{\mathbf{q}, \mathbf{k}, \mathbf{v}} \|\mathbf{y}_t - \hat{\mathbf{y}}_t\|, \quad \text{with} \quad \hat{\mathbf{y}}_t = \frac{\phi(\mathbf{q}_t)^\top \mathbf{H}_t}{\phi(\mathbf{q}_t)^\top \mathbf{s}_t}. \quad (7)$$

After attention distillation, the whole model is finetuned with LoRA [26]. Overall, this procedure only requires 40 million training tokens from the Alpaca dataset [46], grouped in 1024-long sequences.

## 2.4 Disadvantages of Previous Approaches

Even with distillation, linear attention models struggle to accurately mimic the behavior of softmax attention. Initial work in linear attention proposed nonlinear query and key activations to improve the exponential dot product approximation [11, 57]. These methods fall short as they are essentially performing a low-rank approximation of the infinite-rank exponential dot product kernel. In Appendix C, we show that the exponential dot product kernel has slowly decaying singular values for simple data distributions. This implies that high-dimensional hidden states may be required for modest approximation errors.

Recent approaches attempt to address the poor performance of the low-rank approximation in linear attention by augmenting it with sliding window attention [1, 56]. These methods compute a *finite* number of recent tokens in a window with softmax attention and compute the rest with linear attention. Since natural language contains a significant amount of local information, this hybrid approach nearly recovers the performance of pretrained transformers on short-context tasks. For longer sequences, however, these methods struggle to recall important information that falls outside the window and in the hidden state. We show in Table 1 that these models cannot perform associative recall on simple needle-in-a-haystack tasks. Other forms of sparse attention may be required [10].

## 3 Mitigating Memory Collisions with Sparse Caching

Associative memory systems with perfect recall allow stored keys to retrieve their own value. Similar to (4), we use a given key as a query in linear attention’s forward pass to verify this behavior with

$$\frac{\phi(\mathbf{k}_i)^\top \mathbf{H}_t}{\phi(\mathbf{k}_i)^\top \mathbf{s}_t} = \frac{\phi(\mathbf{k}_i)^\top \sum_{j=1}^t \phi(\mathbf{k}_j) \mathbf{v}_j^\top}{\phi(\mathbf{k}_i)^\top \sum_{j=1}^t \phi(\mathbf{k}_j)} = \mathbf{v}_i^\top. \quad (8)$$

In practice, we observe that "memory collisions" often occur. This means non-orthogonal keys interfere with each other when forming the hidden state  $\mathbf{H}_t$ . We define the self-recall score of a given key-value pair as

$$\text{Score}(\mathbf{k}, \mathbf{v} \mid \mathbf{H}_t, \mathbf{s}_t) = \left\| \frac{\phi(\mathbf{k})^\top \mathbf{H}_t}{\phi(\mathbf{k})^\top \mathbf{s}_t} - \mathbf{v} \right\|_2. \quad (9)$$

This determines the error between the predicted value for a given key and the ground truth value. In this work, we demonstrate that a "self-recall check" is useful to see if a key-value pair is properly stored. LoLA uses this scoring approach to decide which KV pairs should be stored separately in full-rank. Large scores indicate the severity of the memory collision. As a result, LoLA maintains the top-scoring KV pairs in a sparse cache. This limits the corruption of past memories and improves associative recall.

**Method Overview.** LoLA addresses the limitations of previous linear attention mechanisms by integrating a sparse caching strategy at inference time. This method employs three memory systems to approximate the softmax kernel effectively and better manage the hidden state

1. **Linear Attention** utilizes a finite-rank approximation to store an infinite amount of generic tokens.
2. **Sliding Window Attention** provides full-rank attention scores for local context.
3. **Sparse Caching** identifies and stores key-value pairs that are challenging to remember, maintaining high-fidelity representations for long-term dependencies.

LoLA mitigates memory collisions by determining which key-value pairs disagree with the current hidden state’s associative map. At every iteration, LoLA scores the KV pair leaving the sliding window and re-scores all pairs in the sparse cache. Re-scoring is needed since the self-recall error is dependent on the current hidden state. A KV pair could become "easier to remember" in the future, after hidden state updates.

We define the pairs that are scored at time  $t$  as

$$\mathcal{E}_t = G_{t-1} \cup \{(\mathbf{k}_{t-\eta}, \mathbf{v}_{t-\eta})\}, \quad (10)$$

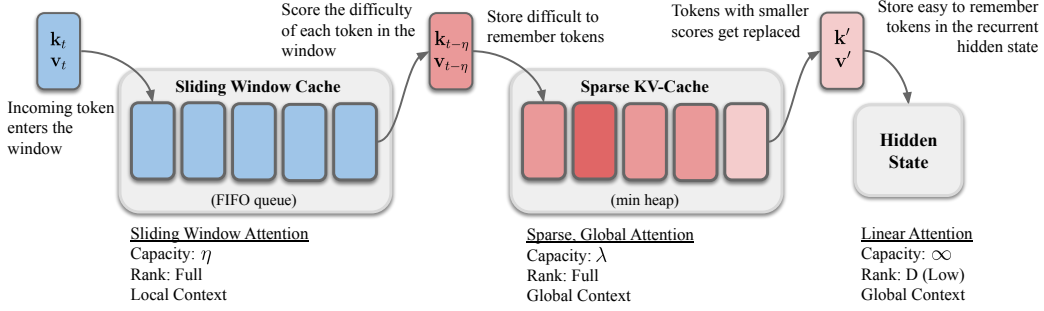


Figure 1: LoLA stores past KV pairs in three forms memory.

where  $G_{t-1}$  is the set of KV pairs in the sparse cache at time  $t-1$ . Also,  $\eta$  is the maximum number of pairs in the sliding window. Then, we update the sparse cache by taking the top- $\lambda$  scoring pairs in  $\mathcal{E}_t$ , i.e.,

$$G_t = \arg \max_{G \subset \mathcal{E}_t: |G|=\lambda} \sum_{(\mathbf{k}, \mathbf{v}) \in G} \text{Score}(\mathbf{k}, \mathbf{v} | \mathbf{H}_t, \mathbf{s}_t). \quad (11)$$

The remaining pairs, denoted by  $\mathcal{S}_t = \mathcal{E}_t \cap G_t^c$  where  $G_t^c$  is the complement of  $G_t$ , are stored in hidden state via

$$\mathbf{H}_t = \mathbf{H}_{t-1} + \sum_{(\mathbf{k}, \mathbf{v}) \in \mathcal{S}_t} \phi(\mathbf{k}) \mathbf{v}^\top, \quad \mathbf{s}_t = \mathbf{s}_{t-1} + \sum_{(\mathbf{k}, \mathbf{v}) \in \mathcal{S}_t} \phi(\mathbf{k}) \quad (12)$$

Once the caches are up to date, LoLA computes the output token  $\mathbf{y}_t$  as

$$\mathbf{y}_t = \frac{\overbrace{\phi(\mathbf{q}_t)^\top \mathbf{H}_t}^{\text{Linear Attn.}} + \overbrace{\sum_{i \in G_t} \exp(\mathbf{q}_t^\top \mathbf{k}_i / \sqrt{d}) \mathbf{v}_i}^{\text{Sparse Cache}} + \overbrace{\sum_{j=t-\eta+1}^t \exp(\mathbf{q}_t^\top \mathbf{k}_j / \sqrt{d}) \mathbf{v}_j}^{\text{Sliding Window}}}{\phi(\mathbf{q}_t)^\top \mathbf{s}_t + \sum_{i \in G_t} \exp(\mathbf{q}_t^\top \mathbf{k}_i / \sqrt{d}) + \sum_{j=t-\eta+1}^t \exp(\mathbf{q}_t^\top \mathbf{k}_j / \sqrt{d})}. \quad (13)$$

Both  $\eta$  and  $\lambda$  are hyper-parameters for the size of the sliding window and sparse cache, respectively.

**Chunkwise Inference.** When the input sequence is available ahead of time (e.g., prefill), LoLA is accelerated with parallelization [52]. By partitioning the input sequence into chunks of size  $C$ , we can compute intra-chunk operations in parallel with dense matmuls. This reduces the number of recurrent iterations by a factor of  $C$  while preserving the constant-memory cost that motivates LoLA.

LoLA computes softmax attention with the current chunk of queries and past two chunks of KV-pairs. For small chunk sizes, softmax attention is almost equally efficient to linear attention. Artificially limiting softmax within a chunk will not improve efficiency, only hurt performance. The past two chunks of KV-pairs are concatenated with the sparse cache in order to compute a single FlashAttention [13] pass per chunk of queries. For the linear attention outputs, all queries within the chunk share the same hidden state.

After computing the past chunk of output tokens, we evict the oldest KV-pairs in the window, sending them to the hidden state or sparse cache. All of the evicted and sparse cache pairs are scored with the self-recall error (9). The  $\lambda$  pairs with the largest errors in the eligible set,

$$\mathcal{E}_t = G_{t-1} \cup \{(\mathbf{k}_i, \mathbf{v}_i) \mid t-2C \leq i < t-C\}, \quad (14)$$

will remain in the sparse cache. The remainder are integrated into the hidden state through the standard outer product update (5).

The given hardware setup dictates the total fixed cache size of LoLA, but the ratio of chunk size to sparse cache size depends on the application. Increasing the chunk size  $C$  reduces the number of recurrent iterations and overhead costs from sparse caching. This puts more emphasis on local KV-pairs since there will be a larger portion of sliding window attention. Increasing the sparse cache size  $\lambda$  will better mitigate collisions in the hidden state and improve long context recall. For simplicity in our recall experiments, we choose  $C = \lambda$  and report various total cache sizes.

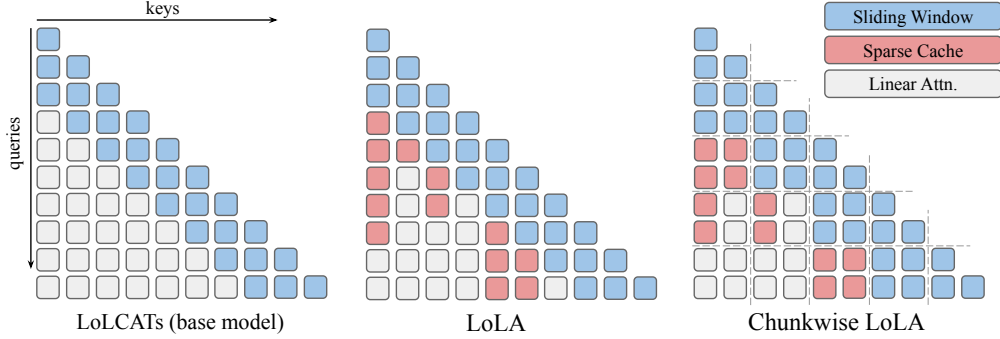


Figure 2: Illustration of where each KV pair is stored at every time step for each method.

## 4 Experiments & Results

In our experiments, we leverage the same attention distillation procedure in LoLCATs to obtain the base model, then apply our inference strategy, LoLA, at test time. To train the baseline model, we replace each attention module in Llama-3.1 8B (or Llama-3.2 1B) with a hybrid sliding window + linear attention module. We use a sliding window size  $\eta = 64$  for training and use a trainable feature map for  $\phi$  as described in (6). Here, the output dimension of  $\phi$  is  $D = 2d$ , where  $d$  is the respective head dimension of the pretrained transformer (e.g.,  $d = 128$  for Llama-3.1 8B). First, we freeze all non-attention layers in the linearized Transformer and only train  $\phi$  with distillation for two epochs on Alpaca. Then, we perform LoRA [26] finetuning on the whole model for another two epochs. This procedure only uses 40M training tokens with 1024-long sequences. For the base LoLA used in Table 1 and 3, we keep LoLCATs’ sliding window size of  $\eta = 64$  and add a sparse cache of size  $\lambda = 64$ . We also provide extended cache sizes in Table 1.

### 4.1 Associative Recall

To see how LoLA improves associative recall, we conduct a study on Single-Needle-in-a-Haystack (S-NIAH) tasks from RULER [25]. In these tasks, the “haystack” is synthetically constructed with various context lengths. The first task, S-NIAH-1, uses random sentences (e.g., “The grass is green.”) as the haystack, while S-NIAH-2 & 3 use essays. The needle—represented as a (word, number) pair—is placed in the haystack. At the end of the prompt, the model is tasked with returning the associated number with the special word. The first two tasks (S-NIAH-1 & 2) use a 7-digit number in the needle, and S-NIAH-3 uses a 32-digit UUID, requiring more tokens to represent the needle.

In our experiment, we ablated extended forms of LoLCATs-8B (i.e extended sliding window, no sparse caching) and LoLA-8B. We provided various total cache sizes, choosing  $C = \lambda$  for simplicity. All extended caches are marked with “+”. Each extension doubles the amount of tokens computed with softmax attention. For a simpler reference, we report the compression rate as the size of Llama-3.1-8B’s cache divided by the total cache size of each method. Since Llama’s cache depends on context length, we report multiple rates.

In Table 1, we observe LoLCATs struggles to recall information outside the sliding window. Extending the sliding window size marginally improves the performance. For large haystacks, the accuracy is roughly the proportion of context that the sliding window covers. For smaller haystacks, the performance is slightly higher than that ratio since fewer pairs stored in the hidden state. This results in fewer collisions. Additionally, we observe that fewer collisions exist in essay-based haystacks (S-NIAH-2 & 3), likely as a result of being more similar to the distillation data.

LoLA drastically improves recall with minimal additional caching. Table 1 demonstrates an improvement from 0.6% to 97.4% accuracy on S-NIAH-1 while still using a  $4.6\times$  smaller cache than Llama. This unlocks a new capability for hybrid linear attention architectures. Our extended results in Table 2 demonstrate recall on up to 8K context length, which is  $8\times$  longer than the sequences seen during training.

Extending the cache size can improve performance while still maintaining high compression rates over transformers. For even longer context lengths, LoLA’s cache can easily be scaled at inference

Table 1: Measuring long context recall with Needle-in-a-Haystack tasks from the RULER benchmark. We report recall accuracy for each method across different context lengths (512, 1024, etc.) for each task.

Model	Compression Rate @ 2-4K	S-NIAH-1				S-NIAH-2			S-NIAH-3		
		.5K	1K	2K	4K	.5K	1K	2K	.5K	1K	2K
<b>Transformer</b>											
Llama-3.1-8B	1×	100	100	100	100	100	100	100	100	100	100
<b>Base Subquadratic Model</b>											
LoLCATs-8B	11×-22×	9.0	3.2	1.4	0.6	100	7.6	2.0	97.4	1.6	0.6
<b>Extended at Inference</b>											
LoLCATs-8B+	6.4×-13×	29.4	9.6	3.4	1.4	100	17.4	7.2	98.2	14.6	3.2
LoLA-8B	6.4×-13×	99.0	95.4	79.4	69.4	100	39.4	3.0	99.8	7.4	1.6
LoLCATs-8B++	4.0×-8.0×	87.2	26.8	10.2	3.2	100	37.0	12.2	100	32.4	6.0
LoLA-8B++	4.0×-8.0×	100	99.6	96.4	89.6	100	98.8	15.0	99.8	33.4	9.2
LoLCATs-8B+++	2.3×-4.6×	100	65.6	24.6	8.8	100	71.8	21.6	100	66.0	10.6
LoLA-8B+++	2.3×-4.6×	100	100	99.6	97.4	100	100	85.4	99.8	99.8	27.2
LoLA-8B++++	1.2×-2.4×	100	100	100	99.0	100	100	100	100	100	100

Table 2: Extended Results on S-NIAH-1. Reported as [Accuracy / Compression Rate]. We evaluated performance across 500 synthetic samples on all context lengths except 16K, which used 250.

Model	.5K	1K	2K	4K	8K	16K
LoLA-8B 4+	100% / 1×	100% / 1×	100% / 1.2×	99.0% / 2.4×	92.2% / 4.9×	13.6% / 9.8×

to achieve the desired recall performance. LoLA is at least as memory-efficient as attention since we can always fall back to softmax attention for short sequences. Lastly, we observe that harder needle-in-a-haystack tasks (e.g., S-NIAH-3 with 32-digit needles) may require more sparse caching. To further extend these results, we believe training with longer sequences should yield stronger performance.

## 4.2 Commonsense Reasoning

We demonstrate the language modeling performance of LoLA on various zero-shot commonsense reasoning tasks using LM evaluation harness [17]. To compare against previously available approaches, we use PIQA (PI) [8], ARC-Easy (AE) & ARC-Challenge (AC) [12], HellaSwag (HS) [55], WinoGrande (WG) [40], MMLU (MM) [23], and Lambada OpenAI [33].

In Table 3, we compare LoLA against other 7-9B *subquadratic* models (Mamba [21], Mamba2 [14], RWKV-6 [35], Hawk & Griffin [15], Falcon Mamba [58], RecurrentGemma [9], Mamba-in-the-Llama [49], Llama [5], Hedgehog [57], and LoLCATs [56]). Models that use any form of unbounded global attention (e.g interleaving SSM blocks and Transformer blocks) still retain quadratic compute complexity and growing memory costs. These are outside the scope of this work. We also report the number of training tokens used to create each model in both tables. Though LoLA is an inference strategy that can be used for any sliding window + linear attention model, we report the cost of distilling the base subquadratic model [56]. In Appendix A, we show results for 1-2B subquadratic models. Additionally, we provide a direct comparison of distilled models by measuring the average accuracy relative to their teacher models.

On short context tasks such as Winogrande, we observe additional caching is not needed as only local information is required for good performance. On the other hand, we find that gaps still exist with Lambada and MMLU. Lambada requires longer context reasoning, leading to significant improvements with sparse caching. Furthermore, Bick et al. [5] suggest that dataset selection plays a large role for MMLU performance. Though sparse caching shows significant improvement on MMLU, a more powerful distillation procedure or dataset may be needed to reach Llama’s performance [19].

For 1B parameter models, sparse caching provides even more utility. Since the hidden state dimensionality scales with the head dimension of the base model, 1B models can face more memory

Table 3: Performance comparison of 7-9B parameter fixed-memory models across various common sense reasoning tasks: PIQA (PI), Arc-Easy (AE), ARC-Challenge (AC), Winogrande (WG), MMLU (MM), and Lambada-openai (LB). Bolded scores are the best and underlined scores are the second best. We report accuracy for all applicable, except AC and HS use normalized logits. MMLU (MM) uses 5-shot. Reported scores were compiled from [5, 48, 49, 56]. \* indicates our reproduced score is used and is higher than reported score.

Model	Tokens (B)	PI	AE	AC	HS	WG	MM	LB
<b>Transformers</b>								
Llama-3.1-8B	15000	<u>81.1</u>	81.7	55.1	79.3	<b>73.9</b>	<b>68.0</b>	<u>73.0</u>
<b>Subquadratic: Pretrained from scratch</b>								
Mamba-8B	1100	78.9	75.4	42.2	75.6	68.3	28.0	-
Mamba2-8B	3500	79.8	75.9	48.1	77.7	71.6	48.7	-
RWKV-6 (W2.1) 7B	1420	78.7	76.8	46.3	75.1	70.0	-	-
Hawk 7B	300	80.0	74.4	45.9	77.6	69.9	35.0	-
Griffin 7B	300	81.0	75.4	47.9	78.6	72.6	39.3	-
Falcon3-Mamba-7B	7300	79.7	72.5	53.2	<u>79.8</u>	69.1	<u>65.0</u>	67.5
RecurrentGemma-9B	2000	80.6	78.9	<b>57.1</b>	<b>80.1</b>	<u>73.7</u>	55.1	54.1
<b>Subquadratic: Distilled from Llama-3.1-8B</b>								
Mamba2-Llama3-8B (L3.1-Instr.)	20	76.8	74.1	48.0	70.8	58.6	43.2	-
Hedgehog-8B (Llama-3)	0.04	77.4	71.1	40.6	66.5	54.3	24.2	-
Llama-8B	12	80.9	<b>82.5</b>	54.6	77.6	73.3	60.0	69.4
LoLCATs-8B	0.04	81.0	82.4	54.4	79.1	73.6*	54.9	67.6
LoLA-8B (ours)	0.04	<b>81.6</b>	<b>82.5</b>	<u>55.4</u>	<u>79.8</u>	73.6	57.6	<b>74.9</b>

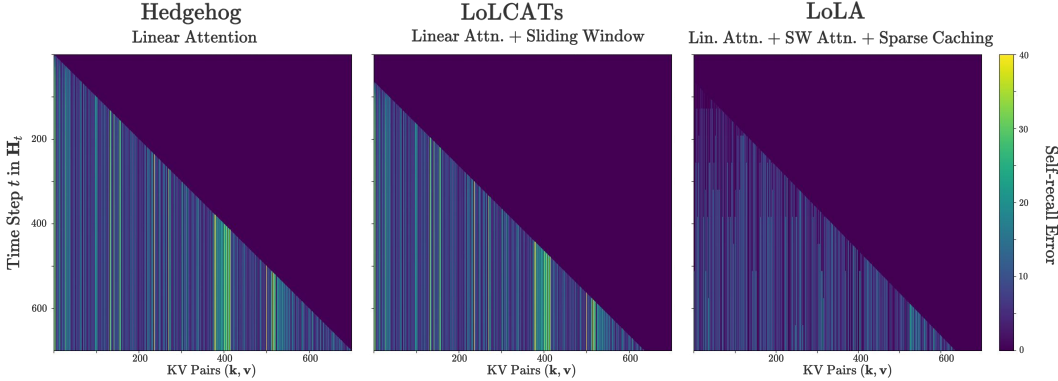


Figure 3: Visualizing memory collisions by measuring self-recall error for stored KV pairs.

collisions. In Appendix A, LoLA demonstrates state-of-the-art performance among 1B subquadratic models, even outperforming Llama-3.2-1B on average. Overall, LoLA pushes the pareto front for training-efficient and high-performing subquadratic LLMs.

### 4.3 Understanding Memory Collisions

We visualize how memory collisions occur in practice. At each time step  $t$ , we measure the self-recall error (9) for every KV pair that is currently stored in the hidden state  $\mathbf{H}_t$ . We visualize the error for linear attention, sliding window + linear attention, and LoLA. We use a sliding window size of  $\eta = 64$  tokens and a sparse cache size of  $\lambda = 64$  when applicable.

When only using linear attention, we observe large recall errors. At early time steps, the first few KV pairs receive small errors, but quickly become larger after hidden state updates. In Appendix E, we additionally plot the relative error to better show how this occurs. These stored associative memories become corrupted and tough to recall in the future. Furthermore, difficult-to-memorize pairs are evident, illustrated as bright columns in Figure 3. The additional use of sliding window attention only delays the inevitable memory collisions.



LoLA significantly reduces the errors for all KV pairs. Difficult-to-memorize pairs are appropriately stored in the sparse cache, as seen by the zero-columns in the plot. This also prevents corrupting older KV pairs that are already stored in the hidden state.

**Scoring Method Ablation.** In our final experiment, we measure alternative scoring functions to understand which KV pairs should be sparsely cached. We provide an informal explanation with each function. Extended details for the score calculation can be found in Appendix D.

Table 4: Ablation results for various scoring methods on S-NIAH-1 with 512 context length.

Alternatives for $\text{Score}(\mathbf{k}, \mathbf{v})$	S-NIAH-1 @ .5K	Informal Assumption for “Important” Pairs
$\left\  \frac{\phi(\mathbf{k})^\top \mathbf{H}}{\phi(\mathbf{k})^\top \mathbf{s}} - \mathbf{v} \right\ $	99.0%	<i>Pairs that do not align with the hidden state’s prediction</i>
$(\exp(\mathbf{q}^\top \mathbf{k}) - \phi(\mathbf{q})^\top \phi(\mathbf{k}))^2$	11.4%	<i>Keys with incorrect attention weights</i>
$ \exp(\mathbf{q}^\top \mathbf{k}) - \phi(\mathbf{q})^\top \phi(\mathbf{k}) $	20.0%	<i>Keys with incorrect attention weights</i>
$\frac{\phi(\mathbf{q})^\top \phi(\mathbf{k})}{\exp(\mathbf{q}^\top \mathbf{k})}$	52.0%	<i>Keys that Linear Attention over estimates</i>
None, extend sliding window	29.4%	<i>Most recent pairs</i>

In Table 4, we observe that storing keys with poor exponential dot product approximations underperforms the naive extension of sliding window attention. This hints that a better softmax approximation should not be the main objective for linear attention methods. Keys over-estimated by linear attention seem to be “more important” than local keys; however, all tested alternatives fall short of enabling associative recall. Overall, our experiments suggest that key-value pairs that are unaligned with the hidden state should be carefully handled.

## 5 Conclusion

LoLA integrates linear attention with sparse caching to effectively mitigate memory collisions. By selectively retaining KV pairs that do not align with the current hidden state, LoLA enables passkey retrieval when the base model fails. Our experimental results demonstrate that targeted sparse caching substantially improves performance over naively increasing sliding window size. LoLA demonstrates strong language modeling performance over other 1B or 8B subquadratic models.

**Limitations and future work.** The sparse cache carries a small overhead compute cost of  $\mathcal{O}(\lambda d)$  for scoring. For high-complexity, long-context tasks, we found that larger sparse cache sizes are needed to reduce interference in the hidden state. We believe that these limitations can be addressed in the future with a better base subquadratic model. More advanced architectures like Gated DeltaNet [51] or Titans [3] use stronger forms of associative memory, which may lead to smaller caches.

## References

- [1] S. Arora, S. Eyuboglu, M. Zhang, A. Timalisina, S. Alberti, J. Zou, A. Rudra, and C. Re. Simple linear attention language models balance the recall-throughput tradeoff. In *International Conference on Machine Learning*, pages 1763–1840. PMLR, 2024.
- [2] M. Beck, K. Pöppel, M. Spanring, A. Auer, O. Prudnikova, M. K. Kopp, G. Klambauer, J. Brandstetter, and S. Hochreiter. xlm: Extended long short-term memory. In *The Thirty-eighth Annual Conference on Neural Information Processing Systems*, 2024.
- [3] A. Behrouz, P. Zhong, and V. Mirrokni. Titans: Learning to memorize at test time. *arXiv preprint arXiv:2501.00663*, 2024.
- [4] I. Beltagy, M. E. Peters, and A. Cohan. Longformer: The long-document transformer, 2020.
- [5] A. Bick, T. Katsch, N. Sohoni, A. Desai, and A. Gu. Llama: Scaling distilled recurrent models for efficient language processing. *arXiv preprint arXiv:2502.14458*, 2025.
- [6] A. Bick, K. Li, E. Xing, J. Z. Kolter, and A. Gu. Transformers to ssms: Distilling quadratic knowledge to subquadratic models. *Advances in Neural Information Processing Systems*, 37:31788–31812, 2024.
- [7] A. Bietti, V. Cabannes, D. Bouchacourt, H. Jegou, and L. Bottou. Birth of a transformer: A memory viewpoint. *Advances in Neural Information Processing Systems*, 36:1560–1588, 2023.
- [8] Y. Bisk, R. Zellers, J. Gao, Y. Choi, et al. Piqa: Reasoning about physical commonsense in natural language. In *Proceedings of the AAAI conference on artificial intelligence*, volume 34, pages 7432–7439, 2020.
- [9] A. Botev, S. De, S. L. Smith, A. Fernando, G.-C. Muraru, R. Haroun, L. Berrada, R. Pascanu, P. G. Sessa, R. Dadashi, et al. Recurrentgemma: Moving past transformers for efficient open language models. *CoRR*, 2024.
- [10] B. Chen, T. Dao, E. Winsor, Z. Song, A. Rudra, and C. Ré. Scatterbrain: Unifying sparse and low-rank attention. *Advances in Neural Information Processing Systems*, 34:17413–17426, 2021.
- [11] K. M. Choromanski, V. Likhoshesterov, D. Dohan, X. Song, A. Kane, T. Sarlos, P. Hawkins, J. Q. Davis, A. Mohiuddin, L. Kaiser, et al. Rethinking attention with performers. In *International Conference on Learning Representations*, 2020.
- [12] P. Clark, I. Cowhey, O. Etzioni, T. Khot, A. Sabharwal, C. Schoenick, and O. Tafjord. Think you have solved question answering? try arc, the ai2 reasoning challenge. *arXiv preprint arXiv:1803.05457*, 2018.
- [13] T. Dao, D. Fu, S. Ermon, A. Rudra, and C. Ré. Flashattention: Fast and memory-efficient exact attention with io-awareness. *Advances in neural information processing systems*, 35:16344–16359, 2022.
- [14] T. Dao and A. Gu. Transformers are SSMs: Generalized models and efficient algorithms through structured state space duality. In *International Conference on Machine Learning (ICML)*, 2024.
- [15] S. De, S. L. Smith, A. Fernando, A. Botev, G.-C. Muraru, A. Gu, R. Haroun, L. Berrada, Y. Chen, S. Srinivasan, et al. Griffin: Mixing gated linear recurrences with local attention for efficient language models. *CoRR*, 2024.
- [16] C. Eckart and G. Young. The approximation of one matrix by another of lower rank. *Psychometrika*, 1(3):211–218, 1936.
- [17] L. Gao, J. Tow, B. Abbasi, S. Biderman, S. Black, A. DiPofi, C. Foster, L. Golding, J. Hsu, A. Le Noac’h, H. Li, K. McDonnell, N. Muennighoff, C. Ociepa, J. Phang, L. Reynolds, H. Schoelkopf, A. Skowron, L. Sutawika, E. Tang, A. Thite, B. Wang, K. Wang, and A. Zou. A framework for few-shot language model evaluation, 07 2024.
- [18] P. Glorioso, Q. Anthony, Y. Tokpanov, J. Whittington, J. Pilault, A. Ibrahim, and B. Millidge. Zamba: A compact 7b ssm hybrid model. *arXiv preprint arXiv:2405.16712*, 2024.
- [19] D. Goldstein, E. Alcaide, J. Lu, and E. Cheah. Radlads: Rapid attention distillation to linear attention decoders at scale. *arXiv preprint arXiv:2505.03005*, 2025.
- [20] A. Grattafiori, A. Dubey, A. Jauhri, A. Pandey, A. Kadian, A. Al-Dahle, A. Letman, A. Mathur, A. Schelten, A. Vaughan, et al. The llama 3 herd of models. *arXiv preprint arXiv:2407.21783*, 2024.
- [21] A. Gu and T. Dao. Mamba: Linear-time sequence modeling with selective state spaces. *arXiv preprint arXiv:2312.00752*, 2024.
- [22] A. Gu, K. Goel, and C. Re. Efficiently modeling long sequences with structured state spaces. In *International Conference on Learning Representations*, 2021.
- [23] D. Hendrycks, C. Burns, S. Basart, A. Zou, M. Mazeika, D. Song, and J. Steinhardt. Measuring massive multitask language understanding. *arXiv preprint arXiv:2009.03300*, 2020.
- [24] G. Hinton, O. Vinyals, and J. Dean. Distilling the knowledge in a neural network. *arXiv preprint arXiv:1503.02531*, 2015.

- [25] C.-P. Hsieh, S. Sun, S. Kriman, S. Acharya, D. Rekesch, F. Jia, Y. Zhang, and B. Ginsburg. Ruler: What’s the real context size of your long-context language models? *arXiv preprint arXiv:2404.06654*, 2024.
- [26] E. J. Hu, Y. Shen, P. Wallis, Z. Allen-Zhu, Y. Li, S. Wang, L. Wang, W. Chen, et al. Lora: Low-rank adaptation of large language models. *ICLR*, 1(2):3, 2022.
- [27] A. Katharopoulos, A. Vyas, N. Pappas, and F. Fleuret. Transformers are rnns: Fast autoregressive transformers with linear attention. In *International conference on machine learning*, pages 5156–5165. PMLR, 2020.
- [28] Y. Li, S. Bubeck, R. Eldan, A. Del Giorno, S. Gunasekar, and Y. T. Lee. Textbooks are all you need ii: phi-1.5 technical report. *arXiv preprint arXiv:2309.05463*, 2023.
- [29] A. Liu, B. Feng, B. Wang, B. Wang, B. Liu, C. Zhao, C. Dengr, C. Ruan, D. Dai, D. Guo, et al. Deepseek-v2: A strong, economical, and efficient mixture-of-experts language model. *arXiv preprint arXiv:2405.04434*, 2024.
- [30] J. Mercat, I. Vasiljevic, S. S. Keh, K. Arora, A. Dave, A. Gaidon, and T. Kollar. Linearizing large language models. In *First Conference on Language Modeling*.
- [31] P. Nawrot, R. Li, R. Huang, S. Ruder, K. Marchisio, and E. M. Ponti. The sparse frontier: Sparse attention trade-offs in transformer llms. *arXiv preprint arXiv:2504.17768*, 2025.
- [32] C. Olsson, N. Elhage, N. Nanda, N. Joseph, N. DasSarma, T. Henighan, B. Mann, A. Askell, Y. Bai, A. Chen, et al. In-context learning and induction heads. *CoRR*, 2022.
- [33] D. Paperno, G. Kruszewski, A. Lazaridou, Q. N. Pham, R. Bernardi, S. Pezzelle, M. Baroni, G. Boleda, and R. Fernández. The lambada dataset: Word prediction requiring a broad discourse context. *arXiv preprint arXiv:1606.06031*, 2016.
- [34] G. Penedo, H. Kydlicek, L. B. Allal, and T. Wolf. Fineweb: Decanting the web for the finest text data at scale. *HuggingFace*. Accessed: Jul, 12, 2024.
- [35] B. Peng, D. Goldstein, Q. G. Anthony, A. Albalak, E. Alcaide, S. Biderman, E. Cheah, T. Ferdinan, K. K. GV, H. Hou, et al. Eagle and finch: Rwkv with matrix-valued states and dynamic recurrence. In *First Conference on Language Modeling*, 2024.
- [36] H. Peng, N. Pappas, D. Yogatama, R. Schwartz, N. Smith, and L. Kong. Random feature attention. In *International Conference on Learning Representations*, 2020.
- [37] Z. Qin, W. Sun, H. Deng, D. Li, Y. Wei, B. Lv, J. Yan, L. Kong, and Y. Zhong. cosformer: Rethinking softmax in attention. In *International Conference on Learning Representations*.
- [38] Z. Qin, S. Yang, W. Sun, X. Shen, D. Li, W. Sun, and Y. Zhong. Hgrn2: Gated linear rnns with state expansion. In *First Conference on Language Modeling*, 2024.
- [39] L. Ren, Y. Liu, Y. Lu, C. Liang, W. Chen, et al. Samba: Simple hybrid state space models for efficient unlimited context language modeling. In *The Thirteenth International Conference on Learning Representations*, 2025.
- [40] K. Sakaguchi, R. L. Bras, C. Bhagavatula, and Y. Choi. Winogrande: An adversarial winograd schema challenge at scale. *Communications of the ACM*, 64(9):99–106, 2021.
- [41] I. Schlag, K. Irie, and J. Schmidhuber. Linear transformers are secretly fast weight programmers. In *International conference on machine learning*, pages 9355–9366. PMLR, 2021.
- [42] J. Siems, T. Carstensen, A. Zela, F. Hutter, M. Pontil, and R. Grazi. Deltaproduct: Increasing the expressivity of deltanet through products of householders. In *ICLR 2025 Workshop on Foundation Models in the Wild*, 2025.
- [43] P. Singhanian, S. Singh, S. He, S. Feizi, and A. Bhatele. Loki: Low-rank keys for efficient sparse attention. In *The Thirty-eighth Annual Conference on Neural Information Processing Systems*, 2024.
- [44] Y. Sun, L. Dong, S. Huang, S. Ma, Y. Xia, J. Xue, J. Wang, and F. Wei. Retentive network: A successor to transformer for large language models, 2023.
- [45] Y. Sun, X. Li, K. Dalal, J. Xu, A. Vikram, G. Zhang, Y. Dubois, X. Chen, X. Wang, S. Koyejo, et al. Learning to (learn at test time): Rnns with expressive hidden states. *arXiv preprint arXiv:2407.04620*, 2024.
- [46] R. Taori, I. Gulrajani, T. Zhang, Y. Dubois, X. Li, C. Guestrin, P. Liang, and T. B. Hashimoto. Stanford alpaca: An instruction-following llama model. [https://github.com/tatsu-lab/stanford\\_alpaca](https://github.com/tatsu-lab/stanford_alpaca), 2023.
- [47] A. Vaswani, N. Shazeer, N. Parmar, J. Uszkoreit, L. Jones, A. N. Gomez, Ł. Kaiser, and I. Polosukhin. Attention is all you need. *Advances in neural information processing systems*, 30, 2017.
- [48] R. Waleffe, W. Byeon, D. Riach, B. Norick, V. Korthikanti, T. Dao, A. Gu, A. Hatamizadeh, S. Singh, D. Narayanan, et al. An empirical study of mamba-based language models. *arXiv preprint arXiv:2406.07887*, 2024.

- [49] J. Wang, D. Paliotta, A. May, A. Rush, and T. Dao. The mamba in the llama: Distilling and accelerating hybrid models. *Advances in Neural Information Processing Systems*, 37:62432–62457, 2024.
- [50] K. A. Wang, J. Shi, and E. B. Fox. Test-time regression: a unifying framework for designing sequence models with associative memory. *arXiv preprint arXiv:2501.12352*, 2025.
- [51] S. Yang, J. Kautz, and A. Hatamizadeh. Gated delta networks: Improving mamba2 with delta rule. *arXiv preprint arXiv:2412.06464*, 2024.
- [52] S. Yang, B. Wang, Y. Zhang, Y. Shen, and Y. Kim. Parallelizing linear transformers with the delta rule over sequence length. In *The Thirty-eighth Annual Conference on Neural Information Processing Systems*, 2024.
- [53] J. Yuan, H. Gao, D. Dai, J. Luo, L. Zhao, Z. Zhang, Z. Xie, Y. Wei, L. Wang, Z. Xiao, et al. Native sparse attention: Hardware-aligned and natively trainable sparse attention. *arXiv preprint arXiv:2502.11089*, 2025.
- [54] M. Zaheer, G. Guruganesh, K. A. Dubey, J. Ainslie, C. Alberti, S. Ontanon, P. Pham, A. Ravula, Q. Wang, L. Yang, et al. Big bird: Transformers for longer sequences. *Advances in neural information processing systems*, 33:17283–17297, 2020.
- [55] R. Zellers, A. Holtzman, Y. Bisk, A. Farhadi, and Y. Choi. Hellaswag: Can a machine really finish your sentence? In *Proceedings of the 57th Annual Meeting of the Association for Computational Linguistics*, 2019.
- [56] M. Zhang, S. Arora, R. Chalamala, A. Wu, B. Spector, A. Singhal, K. Ramesh, and C. Ré. Lolcats: On low-rank linearizing of large language models. In *The Thirteenth International Conference on Learning Representations*, 2025.
- [57] M. Zhang, K. Bhatia, H. Kumbong, and C. Re. The hedgehog & the porcupine: Expressive linear attentions with softmax mimicry. In *The Twelfth International Conference on Learning Representations*, 2024.
- [58] J. Zuo, M. Velikanov, D. E. Rhaïem, I. Chahed, Y. Belkada, G. Kunsch, and H. Hacid. Falcon mamba: The first competitive attention-free 7b language model. *arXiv preprint arXiv:2410.05355*, 2024.

## A Extended Language Modeling Results

**1B parameter model results.** Following Section 4.2, we extend this comparison in Table 5 for various 1-2B parameter subquadratic models [2, 5, 6, 14, 20, 21, 28, 35, 38, 39, 41, 44, 51, 56]. Compared to the 8B models, we observe that sparse caching is more important in the 1B parameter regime since there exist more memory collisions. This is a direct result of a smaller hidden state dimension. The size of  $\mathbf{H}_t$  scales with the head dimension of the base model. Llama-3.2 1B’s head dimension is half that of Llama-3.1 8B.

Table 5: Performance comparison across zero-shot commonsense reasoning tasks for various 1-2B parameter subquadratic models. \* indicates normalized logits were reported instead.

Model	Tokens (B)	PIQA acc $\uparrow$	ARC-e acc $\uparrow$	ARC-c acc_n $\uparrow$	Hella. acc_n $\uparrow$	Wino. acc $\uparrow$	LMB. acc $\uparrow$	LMB. ppl $\downarrow$
<b>Transformers [6, 56]</b>								
Llama-3.2-1B	9000	74.4	65.5	35.8	63.7	60.5	60.1	-
Phi-1.5-1.3B	150	76.6	75.6	48.0	62.6	73.4	53.4	-
<b>Subquadratic: Pretrained from scratch on FineWeb-Edu [34, 51]</b>								
RetNet-1.3B	100	70.1	67.3	33.8	49.2	54.1	40.5	17.3
HGRN2-1.3B	100	70.5	69.4	35.3	49.5	52.8	39.5	17.7
DeltaNet-1.3B	100	70.7	68.5	35.7	50.9	53.4	42.5	16.9
Gated-DeltaNet-1.3B	100	72.3	71.2	38.4	55.8	57.5	46.7	12.2
Mamba1-1.3B	100	71.3	69.5	35.4	52.9	53.0	44.0	15.1
Mamba2-1.3B	100	71.9	72.5	37.9	55.7	55.2	45.7	12.6
<b>Subquadratic: Pretrained from scratch on various sources [5, 6]</b>								
Mamba1-1.4B	315	74.2	65.5	32.8	59.1	61.5	64.9	-
Mamba2-1.3B	315	73.2	64.3	33.3	59.9	60.9	65.7	-
xLSTM-1.4B	300	74.6	64.3	32.6	60.9	60.6	57.8	-
Finch-1.6B	1100	72.6	64.2	34.1	57.3	59.4	66.8	-
RecurrentGemma-2B	2000	67.2	35.6	51.2	60.3	55.7	52.5	-
Samba-1.3B	100	72.4	58.2	-	54.7	55.7	51.7	-
<b>Subquadratic: Distilled from Phi-1.5-1.3B [6, 56]</b>								
Phi-Mamba-1.5B	3	75.5	74.0	44.1	60.2	71.7	50.1	-
LoLCATs-Phi-1.3B	0.04	76.9	77.0	46.9	62.3	72.7	-	-
<b>Subquadratic: Distilled from Llama-3.2-1B [5, 56]</b>								
Llamba-1B	8	74.0*	69.5*	37.2	61.2	60.6	48.4	-
LoLCATs-Llama-1B	0.04	74.6	63.0	35.1	63.7	61.5	53.4	9.3
LoLA-1B (ours)	0.04	76.2	66.2	36.9	64.1	60.9	61.9	5.3

We provide additional notes for the results in Table 5. Mamba and Mamba2 are popular architectures and have been trained many times with different datasets and hyperparameters. We report variations from two sources for robust results. In addition, LoLCATs demonstrated results on both Llama-3.2 1B and Phi-1.5. The model and code for reproducing LoLCATs-Phi-1.3B is not publicly available, so we could not produce Lambada scores. Similarly, we do not have LoLA results for this either. We were able to reproduce LoLCATs-Llama-1B, however, our achieved Winogrande accuracy was lower. We reported the score from the paper, 61.5%, over our reproduced 60.9%.

**Cross-teacher comparison of distilled subquadratic models.** We gathered results from both Table 5 and Table 3 to compare language model performance relative to the teacher models. We average the performance across tasks and compute the relative average. This is calculated by dividing the model’s average by the teacher model’s average.

In Table 6, LoLA outperforms other distilled model approaches. We find that LoLCATs and Llamba perform similarly overall, with LoLCATs demonstrating better token efficiency. Overall, LoLA pushes the pareto front for high-performing and token-efficient models.

Table 6: Comparison of distilled subquadratic models from different teacher models. We report the average accuracy across tasks when applicable (i.e., all scores are reported or available). We also report the relative accuracy, measured as the student average / the teacher average. Results were taken from various related works with the section header containing the sources.

Model	Tokens (B)	PI	AE	AC	HS	WG	LB	Avg.	Rel. Avg.
<b>Transformers</b>									
Phi-1.5-1.3B	150	76.6	75.6	48.0	62.6	73.4	53.4	64.9	-
Llama-3.2-1.3B	9000	74.4	65.5	35.8	63.7	60.5	60.1	60.0	-
Llama-3.1-8B	15000	81.1	81.7	55.1	79.3	73.9	73.0	74.0	-
Llama-3.1-8B-Instr.	15000+	80.8	81.8	55.2	79.2	73.9	-	74.0	-
<b>Subquadratic: Distilled from Phi-1.5-1.3B</b>									
Phi-Mamba1.5B	3	75.5	74.0	44.1	60.2	71.7	50.1	62.6	0.965×
LoLCATs-1.3B	0.04	76.9	77.0	46.9	62.3	72.7	-	-	-
<b>Subquadratic: Distilled from Llama-3.2-1.3B</b>									
Llamba-1.3B	8	74.0*	69.5*	37.2	61.2	60.6	48.4	58.5	0.975×
LoLCATs-1.3B	0.04	74.6	63.0	35.1	63.7	61.5	53.4	58.6	0.977×
LoLA-1.3B (ours)	0.04	76.2	66.2	36.9	64.1	60.9	61.9	61.0	1.017×
<b>Subquadratic: Distilled from Llama-3.1-8B Instruct</b>									
Mamba2-Llama3-8B	20	76.8	74.1	48.0	70.8	58.6	43.2	61.9	0.837×
<b>Subquadratic: Distilled from Llama-3.1-8B</b>									
Llamba-8B	12	80.9	82.5	54.6	77.6	73.3	69.4	73.1	0.987×
LoLCATs-8B	0.04	81.0	82.4	54.4	79.1	73.6	67.6	73.0	0.987×
LoLA-8B	0.04	81.6	82.5	55.4	79.8	73.6	74.9	74.6	1.009×

## B Related Work

In this section, we position LoLA within the broader landscape of subquadratic models and efficient attention mechanisms.

**Linear Attention and State Space Models (SSMs)** State Space Models (SSMs) have emerged as powerful architectures for efficient long-range sequence modeling, offering constant memory complexity irrespective of context length. Pioneered by methods like S4 [22], recent developments include various efficient architectures such as RetNet [44] and Mamba [21]. Concurrently, original linear attention methods have explored efficient approximations of the softmax kernel [11, 27, 36, 37, 57]. Research between SSMs and linear attention has recently converged. Modern SSMs, such as DeltaNet [41], Mamba2 [14] and Gated DeltaNet [51], can be interpreted as linear attention models equipped with additional gating or delta-update mechanisms. Models like DeltaProduct [42] further generalize these linear updates through higher-rank modifications, while Titans [3] and TTT [45] extend the capacity for associative recall using richer hidden-state representations.

Test-time Regression [50] offers a unifying perspective for SSMs and linear attention. These sequence models perform online regression to fit hidden states to past context. Each state update can be interpreted as a gradient step in online SGD. This lens clarifies the roles of different mechanisms within these models. For example, forget gates in Mamba2 and Gated DeltaNet play an analogous role to weight decay. Similarly, momentum-based updates can be overserved in Titans [3].

**Distilling transformers into subquadratic models.** The cost of pretraining LLMs is the primary obstacle in finding the successor of the transformer. To address this issue, recent approaches employ knowledge distillation, transferring the capabilities of pretrained transformers into subquadratic architectures [5, 6, 19, 30, 56]. This significantly reduces training costs by recycling large pretrained models.

MOHAWK [5, 6] demonstrated successful distillation of pretrained transformers into Mamba, maintaining competitive performance. Similarly, “Mamba in the Llama” [49] interleaves transformer and SSM blocks to retain transformer-level performance with significantly reduced inference costs. Though, this approach maintains an unbounded memory footprint due to the residual quadratic attention.

In contrast, LoLCATs use a simpler and cheaper distillation approach by using a student architecture that is more similar to the transformer. The combination of linear attention and sliding window attention significantly reduces the distillation complexity, requiring significantly fewer training tokens. LoLA directly builds on LoLCATs, leveraging its efficient distillation approach while introducing sparse caching to substantially enhance associative recall without extensive retraining.

**Sparse attention methods.** Sparse attention methods present another orthogonal approach to reducing Transformer complexity by limiting the set of attended tokens [31]. Methods such as Longformer [4] and BigBird [54] adopt fixed sparse patterns that incorporate sliding windows and selective global attention, efficiently capturing both local and sparse global contexts. Recent dynamic sparsification approaches, including Loki [43] and Native Sparse Attention (NSA)[53], employ data-dependent strategies, selectively attending to the most relevant tokens based on learned or projected keys. Native Sparse Attention, specifically, combines sparse attention with latent attention mechanisms[29], effectively approximating attention via low-rank and sparse structures.

We believe sparse attention can be complementary to linear attention. With LoLA, we encourage the use of hybrid attention techniques *within* the same attention head. This allows important tokens to leverage more computation when needed. This work contrasts the use of interleaving soft attention blocks with linear attention blocks [18, 39] which allocates the compute costs equally between all tokens.

## C Linear Attention is a Bad Low-Rank Approximation

In this section, we analyze why linear attention struggles to closely approximate softmax attention, specifically highlighting difficulties in approximating the exponential dot product kernel. We start by defining the exponential kernel’s Gram matrix  $\mathbf{G}$  as  $\mathbf{G}_{i,j} = \exp(\mathbf{x}_i^\top \mathbf{x}_j)$  for inputs  $\mathbf{x}_i, \mathbf{x}_j \in \mathbb{R}^d$ . This kernel implicitly corresponds to an inner product in a potentially infinite-dimensional Hilbert space  $\mathcal{H}$  via a feature map  $\phi_{\text{exp}} : \mathbb{R}^d \rightarrow \mathcal{H}$ , such that

$$\exp(\mathbf{x}_i^\top \mathbf{x}_j) = \phi_{\text{exp}}(\mathbf{x}_i)^\top \phi_{\text{exp}}(\mathbf{x}_j). \quad (15)$$

Since explicitly working in an infinite-dimensional space  $\mathcal{H}$  is infeasible, linear attention methods approximate this kernel using a finite-dimensional feature map  $\phi : \mathbb{R}^d \rightarrow \mathbb{R}^D$ . Consequently, linear attention approximates the Gram matrix as

$$\mathbf{G}_{i,j} \approx \hat{\mathbf{G}}_{i,j} = \phi(\mathbf{x}_i)^\top \phi(\mathbf{x}_j), \quad (16)$$

which has a maximum rank of  $D$ . Ideally,  $\hat{\mathbf{G}}$  would closely approximate  $\mathbf{G}$ , minimizing the squared Frobenius norm error. However, linear attention’s approximation error is fundamentally lower-bounded by the truncated singular value decomposition (SVD) of  $\mathbf{G}$  [16]. Specifically, for the SVD decomposition  $\mathbf{G} = \mathbf{U}\mathbf{\Sigma}\mathbf{V}^\top$  with singular values  $\sigma_i$ , we have:

$$\|\mathbf{G} - \hat{\mathbf{G}}\|_F^2 \geq \|\mathbf{G} - \mathbf{U}_D \mathbf{\Sigma}_D \mathbf{V}_D^\top\|_F^2 = \sum_{i=D+1}^{\text{rank}(\mathbf{G})} \sigma_i^2, \quad (17)$$

where  $\mathbf{U}_D \mathbf{\Sigma}_D \mathbf{V}_D^\top$  is the rank  $D$  truncated SVD approximation of  $\mathbf{G}$ .

While the truncated SVD provides the optimal low-rank approximation, it requires the entire Gram matrix to be computed and stored, making it impractical for linear attention which demands computationally efficient, online feature mappings.

To empirically demonstrate the severity of this approximation challenge, we construct the Gram matrix under different input distributions and analyze its singular values. In our simulations, we vary both  $n$  (the number of independently sampled input vectors) and  $d$  (input vector dimensionality) and observe how they affect singular value distributions. Specifically, we draw inputs from a scaled Gaussian distribution  $\mathbf{x}_i \sim \mathcal{N}(0, d^{-1/4})$  to mimic typical transformer scaling of dot products by  $\sqrt{d}$ .

Figures 4 and 5 show that applying an exponential operation to the query-key products significantly increases the rank and complexity of the resulting Gram matrix. The singular values and approximation error increase with the number of unique input vectors  $n$  (see Figure 4) and the input dimension  $d$  (see Figure 5). Practically, in transformer architectures, head dimensions are typically modest

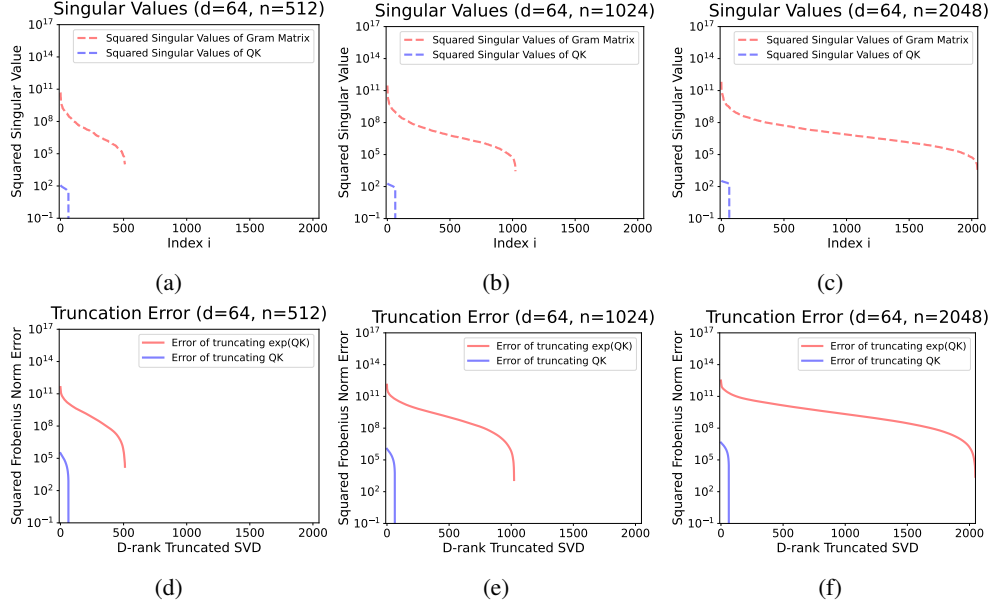


Figure 4: Visualization of singular values of the Gram matrix and minimum squared Frobenius norm error for linear attention (17). We vary the number of i.i.d. vectors  $n$  used to construct the Gram matrix, but maintain the same input dimension  $d$ .

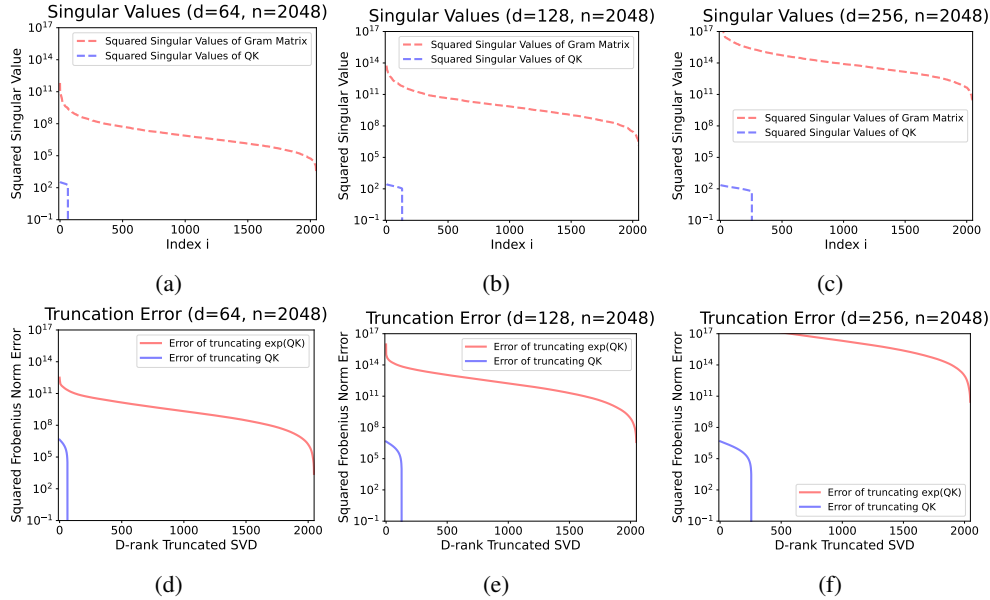


Figure 5: Visualization of singular values of the Gram matrix and minimum squared Frobenius norm error for linear attention (17). We vary the input dimension  $d$  between columns in the plot.

( $d = 64$  for Llama-3.2 1B and  $d = 128$  for Llama-3.1 8B). Additionally, linear attention approaches typically select feature dimensions  $D$  around  $2d$  [56, 57] which can be problematic without additional sparse attention or gating mechanisms.

These experiments underscore the inherent limitation of linear attention as a softmax replacement. For an arbitrarily large vocabulary size, a high dimensional hidden state is needed to truly mimic softmax. We argue that future research should exploit the inherent strengths of linear attention when it makes sense to (e.g., applying linear attention on easier-to-remember tokens), rather than attempting to replicate softmax attention in all situations.



## D Scoring Ablation Extension

In section 4.3, we ablated different scoring approaches for the sparse cache. Here, we describe exactly how each alternative score is computed. As a reminder, LoLA is motivated by the occurrence of memory collisions in the hidden state. LoLA explicitly attempts to maintain self-recall for stored key-value pairs. An alternative perspective could be aiming for the best softmax approximation. Similar to previous kernel work [11], this aims to minimize the attention weight error

$$\sum_i^N \sum_j^N (\exp(\mathbf{q}_i^\top \mathbf{k}_j) - \phi(\mathbf{q}_i)^\top \phi(\mathbf{k}_j))^2. \quad (18)$$

A natural scoring method for this objective would be to keep the keys with the highest attention weight error. As a proxy for this approach, each key’s error can be summed over all queries it sees in the sliding window with

$$\text{Score}(\mathbf{k}_i) = \sum_{t=i}^{i+\eta-1} (\exp(\mathbf{q}_t^\top \mathbf{k}_i) - \phi(\mathbf{q}_t)^\top \phi(\mathbf{k}_i))^2. \quad (19)$$

Alternatively, we can use absolute error over mean squared error instead.

From a third perspective, keys that are over-represented by linear attention’s query-key interactions may seem important to cache. We compute these as

$$\text{Score}(\mathbf{k}_i) = \sum_{t=i}^{i+\eta-1} \frac{\phi(\mathbf{q}_t)^\top \phi(\mathbf{k}_i)}{\exp(\mathbf{q}_t^\top \mathbf{k}_i)}. \quad (20)$$

Lastly, we compare these methods against a larger sliding window.

## E Extended Memory Collision Visualization

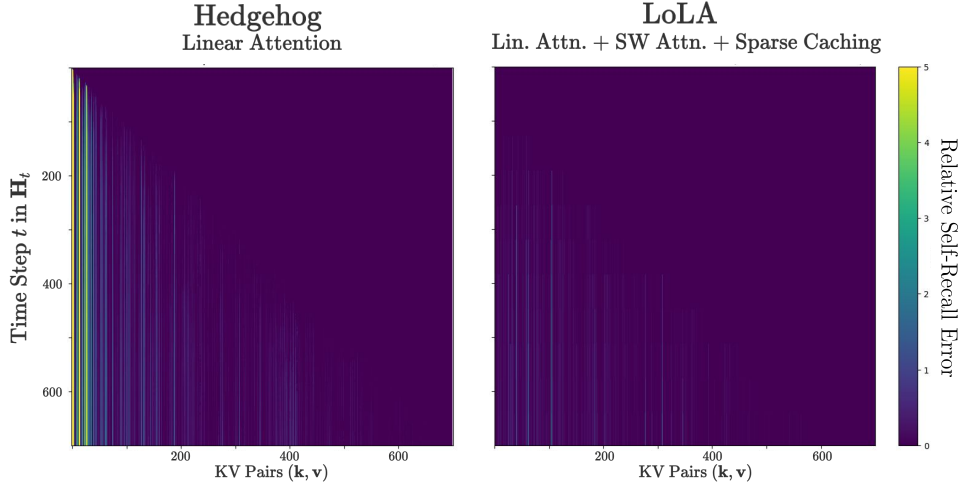


Figure 6: Visualizing the relative self-recall error for stored KV pairs.

In Section 4.3, we visualized how memory collisions can occur in practice. This was computed by measuring the self-recall error for all stored KV pairs. We found that the first few stored KV pairs do not achieve a large error when added to the hidden state. However, these quickly become corrupted after hidden state updates. This phenomenon was difficult to see in Figure 3, so we provide an additional visualization with Figure 6. Specifically, we measure the self-recall error of each KV pair, relative to the error of when that pair was added. For row  $i$  column  $j$  in the plot, the relative error is computed as

$$\left\| \frac{\phi(\mathbf{k}_j)^\top \mathbf{H}_i}{\phi(\mathbf{k}_j)^\top \mathbf{s}_i} - \mathbf{v}_j \right\|_2 - \left\| \frac{\phi(\mathbf{k}_j)^\top \mathbf{H}_t}{\phi(\mathbf{k}_j)^\top \mathbf{s}_t} - \mathbf{v}_j \right\|_2. \quad (21)$$

where  $t$  is the time pair  $j$  was added to the hidden state. Thus, we have  $j \leq t \leq i$ .

Here, we see the first few KV pairs have high relative errors for pure linear attention. These pairs observe small self-recall errors at early time steps, but achieve much higher self-recall errors later. On the other hand, sparse caching actively mitigates self-recall errors, improving associative recall for stored KV pairs.

## F Extended Long Context Tasks

To further extend our results on long-context recall tasks, we report scores for the rest of the RULER benchmark [25] in table 7. These represent harder, multi-step tasks: Needle-in-a-Haystack-style Multi-Key Retrieval (MK1, MK2, MK3), NIAH-style Multi-Query (MQ), NIAH Multi-Value (MV), Variable Tracking (VT), Commonword Extraction (CWE), Frequent Word Extraction (FWE), HotpotQA, and SquadQA. Due to the difficulty of these tasks, we benchmark LoLA on 2048 sequence lengths when applicable. Otherwise, we use the default 4096.

Table 7: Extended results on the RULER benchmark. LoLA 4+ uses chunkwise inference with  $C = \lambda = 512$ , similar to Table 2.

Task Seq. Len	MK1 2K	MK2 2K	MK3 2K	MQ 2K	MV 2K	VT 4K	CWE 4K	FWE 4K	HotpotQA 4K	SquadQA 4K
LoLA 4+	70.0	20.2	0	62.75	54.15	8.3	1.9	12.93	25.2	51.7

## G Algorithm Psuedo-code

We provide PyTorch-like pseudo-code for the cache during decoding or generation. In this example, we update the cache every iteration (rather than chunkwise inference) for simplicity. Lastly, this psuedo-code does not contain any optimization tricks for ease of understanding.

*#Simplified LoLA Cache for Decoding:*

```

class LoLA_Cache:
    def init():
        #Cache for Sliding Window Attention
        local_cache = {keys:[], values:[]} #max size  $\eta$ 

        #Cache for Sparse Attention
        global_cache = {keys:[], values:[]} #max size  $\lambda$ 

        #"Cache" for Linear Attention
        H, s = zeros(D,d), zeros(D)

    #Update memory systems with an incoming KV pair
    def update(k, v):
        eligible_keys = concat(global_cache.keys, k)
        eligible_values = concat(global_cache.values, v)

        #Predict the associated value of each key
        predicted_v = (phi(eligible_keys) @ H) / (phi(eligible_keys) @ s)
        scores = L2_norm(eligible_values - predicted_v)

        #Add min scoring KV pair to hidden state
        min_idx = argmin(scores)
        min_k = eligible_keys[min_idx]
        min_v = eligible_values[min_idx]
        H = H + phi(min_k) @ min_v.T
        s = s + phi(min_k)

        #Update Global Cache as all other KV pairs
        global_cache.keys = eligible_keys[not min_idx]
        global_cache.values = eligible_values[not min_idx]

```

```

#Return the output associated with the query.
def attend(q):
    global_weights = exp(q @ global_cache.keys / sqrt(d) )
    local_weights = exp(q @ local_cache.keys / sqrt(d) )

    unnormalized_attn = sum(global_weights * global_cache.values)
                      + sum(local_weights * local_cache.values)
                      + phi(q) @ h #linear attn

    normalizing_const = sum(global_weights)
                      + sum(local_weights)
                      + phi(q) @ s #linear attn

    return unnormalized_attn / normalizing_const

```